The Meteoritical Society

Meteoritics & Planetary Science 43, Nr 8, 1333–1350 (2008)
Abstract available online at http://meteoritics.org

Noble gas content and isotope abundances in phases of the Saint-Aubin (UNGR) iron meteorite

Chikako NISHIMURA[1*], Jun-ichi MATSUDA[1], and Gero KURAT[2]

[1]Department of Earth and Space Science, Graduate School of Science, Osaka University, Toyonaka, Osaka 560-0043, Japan
[2]Department of Lithospheric Sciences, University of Vienna, Althanstrasse 14, 1090 Vienna, Austria
[*]Corresponding author. E-mail: GZZ03435@nifty.com

(Submitted 18 July 2007; revision accepted 10 February 2008)

Abstract–We analyzed the noble gas isotopes in the Fe-Ni metal and inclusions of the Saint-Aubin iron meteorite, utilizing the stepwise heating technique to separate the various components of noble gases.

The light noble gases in all samples are mostly cosmogenic, with some admixture from the terrestrial atmosphere. Total abundances of noble gases in metal are one of the lowest found so far in iron meteorites and the $^{4}He/^{21}Ne$ ratio is as high as 503, suggesting that the Saint-Aubin iron meteorite was derived from a very large meteoroid in space. The exposure ages obtained from cosmogenic ^{3}He were 9–16 Ma.

Saint-Aubin is very peculiar because it contains very large chromite crystals, which—like the metal—contain only cosmogenic and atmospheric noble gases. The noble gases in all the samples do not reveal any primordial components. The only exception is the 1000 °C fraction of schreibersite which contained about 5% of the Xe-HL component. The Xe-Q and the El Taco Xe components were not found and only the Xe-HL is present in this fraction. Some presolar diamond, the only carrier for the HL component known today, must have been available during growth of the schreibersite. However, it is also possible that this excess is due to the addition of cosmogenic and fission components. In this case, all the primordial components are masked (or lost) by the later events such as cosmic-ray irradiation, heating, and radioactive decay.

INTRODUCTION

Iron meteorites are differentiated meteorites and are generally supposed to be samples of the core of a parent body of differentiated meteorites. The iron meteorites are classified into 12 groups from Ni and trace elements (Ga, Ge, and Ir) content (Scott and Wasson 1975). Some of the 12 groups show correlations of Ni and trace element content that are consistent with formation by fractional crystallization and are considered to form "magmatic" groups. The other iron meteorites are regarded as "non-magmatic." Iron meteorites of this group show several lines of evidence that these metals were not completely melted in the parent body.

Noble gases are chemically inert and volatile, and their elemental abundances and isotopic ratios have been used as good tracers to study the origin and evolution of our solar system. Unfortunately, iron meteorites contain very small amounts of primordial noble gases that are generally masked by large amounts of noble gases produced by cosmic ray irradiation. However, it is expected that some of the inclusions in non-magmatic iron meteorites retain the primordial components such as those observed in primitive undifferentiated chondrites. In this concept, the noble gases in non-magmatic iron meteorites (IAB, IIICD, and IIE) have been widely studied for the last 40 years. Alexander and Manuel (1968) and Bogard et al. (1971) found that silicate inclusions in IAB iron meteorites contained the planetary noble gases observed in carbonaceous chondrites. Mathew and Begemann (1995) reported a new primordial component named "El Taco Xe" in graphite inclusions in the El Taco mass of the Campo del Cielo IAB iron meteorite. The presence of El Taco Xe was further confirmed in graphite inclusions of other IAB iron meteorites such as Bohumilitz (Maruoka et al. 2001) and Canyon Diablo (Matsuda et al. 2005). Maruoka et al. (2001) further reported the presence of Q (a component with normal isotopic ratios but enriched in heavy noble gases) in graphite of Bohumilitz. Matsuda et al. (2005) reported the presence of HL (a component with anomalous isotopic ratios carried by presolar diamond) in addition to Q in a Canyon Diablo graphite nodule. These results show that presolar grains apparently survive iron meteorite formation.

Recent studies of Hf-W isotopes in iron meteorites show that the silicate-metal segregation occurred at a very early stage of the solar system and that the formation of magmatic iron meteorites took place before that of the non-magmatic group (Kleine et al. 2005; Scherstén et al. 2006). Thus, it is very likely that presolar grains have been included even in magmatic-group iron meteorites. Although the thermal event of segregation of metal from silicates in the magmatic group might destroy such signatures of primordial components of noble gases, it might be possible to detect them in some inclusions.

The Saint-Aubin iron meteorite was found on a farm in Aube Champagne, France, in 1968 (Koblitz 2003; Russell et al. 2003). It is an octahedrite with a fine (0.4 mm) Widmanstätten pattern and is chemically classified as an ungrouped iron (Dransart and Baron 2003). Saint-Aubin contains a variety of inclusions: iron phosphate (sarcopside or graftonite), sulfide, needles of schreibersite up to 10 cm in length, and giant euhedral chromite of ~3 cm in size (Fehr and Carion 2004; Kurat et al. 2005).

Chromite in iron meteorites is usually small (10–100 μm). Chromite with a size of ~0.8 mm in the Landes IAB octahedrite has been known as one of the largest chromite crystals in an iron meteorite (Bunch et al. 1972). Thus the large size of the chromite in Saint-Aubin is very unusual. Saint-Aubin is regarded as a magmatic iron meteorite because the composition of the chromite inclusion is similar to pure $FeCr_2O_4$ and slow cooling would be required to produce such a pure chromite (Ulff-Møller 1998; Fehr and Carion 2004). Furthermore, Kurat et al. (2005) determined the major, minor and trace element contents of the chromite and found that it is very poor in lithophile and siderophile elements (only ~600 ppm Mg, 0.4 ppm Al, 1.8 ppm Ni), Sc and REE. Therefore, they concluded that the chromite must have formed in an environment that was very poor in lithophile elements, except Mn, which is abundant in all phases (contrary to the findings of Fehr and Carion 2004). Moreover, Ni is depleted but V is enriched in chromite, which has been interpreted to indicate formation of chromite from a reduced precursor phase in equilibrium with metal (Kurat et al. 2005). It is likely that Fe-phosphates were also formed in a similar way, but early in the history of the solar system because they contain excess ^{53}Cr (possibly from short-lived $^{53}Mn - t_{1/2} = 3.7$ Ma).

In this study, we report the noble gas concentrations and isotopic ratios in metal, chromite, troilite, and schreibersite in the Saint-Aubin (UNGR) iron. Chromite was once supposed to be a candidate host phase of primitive noble gases (Srinivasan et al. 1975; Gros and Anders 1977; Lewis et al. 1977). However, later works showed that chromite was not the host phase of primitive noble gases (Ott et al. 1981). As there is a primitive signal in Saint-Aubin Fe phosphates, this study was undertaken to characterize the noble gas composition in metal and inclusions and determine also its cosmic-ray exposure history.

SAMPLES AND METHODS

The Fe-Ni metal and several inclusions (chromite, troilite, and schreibersite) from the Saint-Aubin iron meteorite were analyzed for their noble gases using a sector-type mass spectrometer (VG5400) at the Osaka University. The inclusion samples were mechanically separated from the sliced sample without acid, etc., and were granular with a few mm or less in size. The granular chromite was named as samples "CR-2" (0.0887 g), "CR-3" (0.135 g), and "CR-4" (0.148 g), troilite was "TR" (0.130 g), and schreibersite was "SC" (0.121 g). A metal nodule was named sample "M" (0.871 g). The granular inclusion samples were wrapped in aluminum foil and baked at 150 °C overnight in the vacuum line.

All samples were stepwise heated in molybdenum crucibles and gases were extracted with a Ta heater. Samples CR-2, TR, and SC were heated in steps of 200 °C from 600 to 1600 °C. Samples CR-3 and CR-4 were heated in steps of 400 °C from 600 or 800 °C to 1800 °C. Sample M was heated in two steps, 600 and 1600 °C. Samples were kept at the extraction temperature for 20 min. It is expected that the noble gases from each temperature fraction are released from different minor sites and/or by diffusion. The extracted gas from the sample was introduced into the purification line. Activated gases were purified with two Ti-Zr getters at 700 °C. The purified gas was led to the cryogenic cold trap for noble gas separation. Each noble gas was separated using the cryogenic trap at 18 K for He, 35 K for Ne, 75 K for Ar, 110 K for Kr, and 183 K for Xe. The elemental abundances and the isotopic ratios of noble gases were then measured with a VG5400 sector-type mass spectrometer. The detector for ^4He and ^{40}Ar was a Faraday collector with a resolution of $M/\Delta M \sim 200$, and that for other isotopes was an ion counting system equipped with a secondary electron multiplier with a resolution of $M/\Delta M \sim 600$. During the He and Ne measurements, the residual heavy noble gases (Ar, Kr, and Xe) were removed using a charcoal trap at the temperature of liquid nitrogen (~77 K). The detailed experimental descriptions can be found in our previous works (e.g., Matsuda et al. 1989; Wada and Matsuda 1998).

An air standard for the sensitivity and the mass discrimination was measured before and after the sample measurement. We used the average of the sensitivity and the mass discrimination factors during the period of each sample measurement because their variation was <1% during the period. An artificial reference HESJ ($^3He/^4He = 2.86 \pm 0.045 \times 10^{-5}$) was used as the $^3He/^4He$ standard (Matsuda et al. 2002), because the amount of ^3He in terrestrial air is too low for a precise determination of the $^3He/^4He$ ratio.

Hot blanks were measured at two or three temperature steps before each sample analysis. The ^4He, ^{22}Ne, ^{36}Ar, ^{84}Kr, and ^{132}Xe blanks are $\sim10^{-10}$, $\sim10^{-13}$, 10^{-12} to 10^{-11}, $\sim10^{-13}$, and $\sim10^{-13}$ cm^3STP, respectively.

RESULTS AND DISCUSSION

The obtained results are given in Tables 1 to 3 where "n.d." denotes "not determined," mainly because of the low amounts of noble gases present. The uncertainties shown in tables and figures are 1σ but include all the error of blank correction and discrimination correction. The errors of Ne isotopic ratios also include the error due to the complicated correction of the interference. The concentrations of ^{4}He, ^{21}Ne, and ^{38}Ar in the metal of Saint-Aubin are very low in comparison with those measured in other iron meteorites: $5.91 \pm 0.37 \times 10^{-7}$, $1.17 \pm 0.07 \times 10^{-9}$, and $6.55 \pm 0.29 \times 10^{-9}$ cm^{3}STP/g, respectively. Consequently, the pre-atmospheric size of Saint-Aubin was likely very large. Canyon Diablo, Odessa, or Acuña, etc., with >5000 kg of pre-atmospheric mass have light noble gas abundances comparable to what we see in Saint-Aubin. The ^{4}He/^{21}Ne ratio is as high as 503, which projects far to the right side of the 10000 kg mass in the production rate P_{21} versus ^{4}He/^{21}Ne plot of Voshage (1984).

In all samples, atmospheric contamination during sample preparation would be released in initial step heating (600 or 800 °C). The high ^{3}He/^{4}He ratios (mostly $>10^{-1}$) of all samples compared to terrestrial air (1.39×10^{-6}) or the trapped component ($\sim 10^{-4}$) show that He is an almost pure cosmogenic component. Also, almost all Ne is of cosmogenic origin, with only small amounts of a trapped component and/or air (Fig. 1). Most Ar appears to be a mixture of air and the cosmogenic component (Fig. 2). Krypton and xenon data are close to the terrestrial air values, but some interesting features are observed in some temperature fractions from troilite and schreibersite. We will address this issue later after discussing the cosmogenic component that is the main component of noble gases in Saint-Aubin.

Cosmogenic Light Noble Gases and Cosmic-Ray Exposure Ages

The light noble gases (He, Ne, and Ar) of all phases are enriched in the cosmogenic component. All ^{3}He in iron meteorites is regarded to be cosmogenic, as stated before. In metal, almost all ^{4}He, ^{21}Ne, and ^{38}Ar is regarded as cosmogenic component (Tables 1 to 3; Figs. 1 and 2). In inclusion samples, it is difficult to distinguish trapped components of Ne (solar wind, terrestrial atmosphere, and Ne-HL) because the errors of the ^{21}Ne/^{22}Ne ratios are large. The cosmogenic ^{21}Ne in chromite, troilite, and schreibersite were estimated as the mixing of terrestrial atmosphere and cosmogenic component. The cosmogenic ^{38}Ar in each inclusion was estimated on the assumption that only two components (cosmogenic and atmospheric) are involved.

The production rates of cosmogenic nuclides (especially Ne) in iron meteorites are less understood than in stony meteorite and their estimations are difficult. The production of cosmogenic Ne is very sensitive to contributions from S- and P-rich inclusions (Ammon and Leya 2007; Ammon et al. 2007) and $(^{22}\text{Ne}/^{21}\text{Ne})_C$ that is used for shielding condition is very sensitive to the matrix and different in stony and iron meteorites (Jentsch and Schultz 1996; Leya et al. 2004). Thus we gave up to get the production rate of ^{21}Ne as the cross section data on Cr does not exist and the shielding correction gave large changes of the production rate value, but we tried to estimate the production rates of ^{3}He according to the equation of Eugster and Michel (1995).

We measured the chemical composition of each phase by EDX analyses and applied the equation of Eugster and Michel (1995) to calculate the production rates. The ^{3}He production rate P_3 was calculated by the equation

$$P_3 = 0.62P'_3[2.09\text{-}0.43(^{22}\text{Ne}/^{21}\text{Ne})_C] \quad (1)$$

where

$$P'_3 = 1.15\ (\text{Ti} + \text{Cr} + \text{Mn} + \text{Fe} + \text{Ni}) + 1.75\ (100 - [\text{Ti} + \text{Cr} + \text{Mn} + \text{Fe} + \text{Ni}])$$

The P_3 is the production ratio corrected by the shielding effect. The obtained P'_3 and P_3 are listed in Table 4. As shown in Table 4, the differences of P_3' and P_3 are only 5%. The obtained production rate P_3 for chromite is 1.33×10^{-8} cm^{3}STP/g per Ma that agrees well with $(1.23 \pm 0.49) \times 10^{-8}$ cm^{3}STP/g per Ma found by Heck et al. (2004), but is slightly smaller than that reported by Heck et al. (2005): $(1.86 \pm 0.10) \times 10^{-8}$ cm^{3}STP/g per Ma. The obtained exposure ages for individual phases agree well with each other and range from 9 to 16 Ma, although schreibersite gives slightly low values, which is not essential when we consider the uncertainty of the production rates.

The obtained exposure ages of Saint-Aubin are lower than the common ages (>100 Ma) observed in iron meteorites.

Isotopic Composition of Noble Gases in Metal and Chromite

Noble gases in Saint-Aubin metal and chromite are dominated by the cosmogenic component.

The isotopic composition of light noble gases in Saint-Aubin chromite indicates admixture of terrestrial air to the cosmogenic component, but is dominated by the cosmogenic component. The cosmogenic Ne and Ar in chromite was 97 and 30% (sample CR3), and 97 and 51% (sample CR4) of the total abundances, respectively. These fractions of cosmogenic components were lower than those in metal (~100% for Ne and 95% for Ar). The cosmogenic ^{21}Ne/^{22}Ne ratio of chromite is larger than that of the metal. The difference of cosmogenic isotopic ratios between the mineral samples is caused by the different production rate of Ne isotopes from the elements present in each phase.

On the other hand, the isotopic composition of Kr and Xe in chromite is, within errors, near the terrestrial

Table 1. Concentrations and isotopic compositions of He, Ne, and Ar in inclusions and metal phase of the Saint-Aubin iron meteorite.

Sample weight (g)	Temp. (°C)	[^{4}He] (10^{-8} cm^3 STP/g)	^{3}He/^{4}He	[^{22}Ne] (10^{-10} cm^3 STP/g)	^{20}Ne/^{22}Ne	^{21}Ne/^{22}Ne	[^{36}Ar] (10^{-10} cm^3 STP/g)	^{38}Ar/^{36}Ar	^{40}Ar/^{36}Ar
Chromite									
CR2	600	<1.43	n.d.	<0.060	n.d.	n.d.	0.8	0.236	330
(0.0887)							±.03	±.003	±5
	800	5.62	0.167	0.052	<7.763	1.06	0.7	0.262	324
		±.23	±.004	±.013		±.548	±.03	±.004	±6
	1000	75.9	0.162	3.97	0.905	0.946	4.1	0.249	314
		±3.0	±.004	±.19	±.073	±.018	±.2	±.001	±5
	1200	31.1	0.166	3.44	0.924	0.924	2.2	0.867	189
		±1.2	±.004	±.16	±.093	±.014	±.1	±.005	±3
	1400	18.6	0.168	3.03	1.054	0.933	8.1	1.520	<134
		±.7	±.004	±.14	±.178	±.018	±.3	±.006	
	1600	5.50	0.17	1.91	1.409	0.895	12.4	1.451	70
		±.23	±.004	±.09	±.269	±.028	±.5	±.005	±1
	Total	136.7	0.164	12.40	1.020	0.929	28.4	1.187	108
		±3.4	±.002	±.30	±.069	±.010	±.6	±.003	±1
CR3	800	26.0	0.156	0.26	2.887	0.758	59.3	0.195	291
(0.1345)		±.3	±.005	±.02	±.279	±.037	±6.2	±.007	±34
	1200	89.6	0.163	8.61	0.932	0.912	6.7	0.971	172
		±.9	±.006	±.57	±.022	±.012	±.7	±.005	±19
	1600	11.8	0.146	2.48	1.236	0.875	12.0	1.499	66
		±.1	±.005	±.16	±.091	±.017	±0.2	±.007	±7
	1800-1	3.1	0.140	1.51	1.183	0.879	11.1	1.497	68
		±.04	±.005	±.10	±.146	±.021	±1.1	±.007	±7
	1800-2	<1.2	n.d.	0.40	1.578	0.815	4.7	1.474	<159
				±.03	±.495	±.053	±.5	±.008	
	1800-3	<1.1	n.d.	0.24	1.850	0.791	3.8	1.485	<175
				±.02	±.774	±.081	±.4	±.009	
	Total	130.6	0.16	13.5	1.089	0.893	97.5	0.668	224
		±.9	±.004	±.6	±.034	±.009	±6.4	±.005	±23
CR4	600	2.52	0.027	0.022	17.831	n.d.	30.9	0.204	319
(0.1482)		±.19	±.002	±.0035	±3.739		±3.8	±.002	±3
	1000	96.16	0.169	8.12	0.873	0.922	3.2	0.499	278
		±6.89	±.003	±.60	±.017	±.010	±.2	±.002	±2
	1400	22.74	0.157	3.30	1.190	0.900	14.4	1.432	77.9
		±1.63	±.003	±.24	±.079	±.012	±1.0	±.002	±.4
	1800-1	5.44	0.143	2.64	1.164	0.876	22.6	1.567	52.3
		±.39	±.003	±.20	±.099	±.014	±1.6	±.002	±.3
	1800-2	<0.77	n.d.	0.27	1.380	0.896	5.2	1.745	<113.7
				±.02	±.848	±.086	±.4	±.006	
	1800-3	<0.71	n.d.	0.20	2.841	0.784	2.0	2.107	<199.4
				±.20	±.958	±.100	±.1	±.015	
	1800-4	<0.70	n.d.	0.10	4.350	0.943	<2.39	n.d.	n.d.
				±.01	±1.388	±.210			
	Total	126.86	0.162	14.65	1.081	0.907	78.3	0.986	183.4
		±7.09	±.003	±.68	±.035	±.007	±4.3	±.001	±1.3
Troilite TR									
(0.1299)	600	1.77	0.131	3.00	1.001	0.770	1.4	0.368	309
		±.08	±.006	±.17	±.012	±.027	±.1	±.002	±6
	800	3.21	0.127	6.25	0.873	0.775	0.62	1.493	812
		±.14	±.005	±.35	±.007	±.017	±.03	±.011	±15
	1000	36.6	0.128	22.0	0.829	0.774	4.9	1.289	787
		±1.5	±.005	±1.2	±.006	±.012	±.2	±.004	±14

Table 1. *Continued.* Concentrations and isotopic compositions of He, Ne, and Ar in inclusions and metal phase of the Saint-Aubin iron meteorite.

Sample weight (g)	Temp. (°C)	[^{4}He] (10^{-8} cm^3 STP/g)	^{3}He/^{4}He	[^{22}Ne] (10^{-10} cm^3 STP/g)	^{20}Ne/^{22}Ne	^{21}Ne/^{22}Ne	[^{36}Ar] (10^{-10} cm^3 STP/g)	^{38}Ar/^{36}Ar	^{40}Ar/^{36}Ar
	1200	88.4	0.130	88.6	0.805	0.780	15.0	1.634	173
		±3.7	±.005	±5.0	±.005	±.012	±.6	±.005	±3
	1400	5.53	0.126	14.5	0.876	0.772	5.0	1.68	<116
		±.24	±.005	±.82	±.010	±.012	±.2	±.007	
	1600	<1.07	n.d.	0.92	1.215	0.692	<2.28	n.d.	n.d.
				±.05	±.088	±.057			
	Total	135.5	0.129	135.3	0.827	0.777	26.9	1.509	336
		±4.0	±.004	±5.2	±.003	±.008	±.7	±.003	±4
Schreibersite SC									
(0.1214)	600	<0.96	n.d.	<0.60	n.d.	n.d.	83.4	0.1879	318
							±4.0	±.0002	±1
	800	2.93	0.179	<0.70	n.d.	n.d.	41.7	0.1909	322
		±.30	±.007				±2.0	±.0003	±2
	1000	13.53	0.217	13.28	0.948	0.824	115.5	0.2219	304
		±1.38	±.008	±.68	±.093	±.083	±5.5	±.0003	±1
	1200	29.85	0.217	37.40	0.757	0.784	61.5	0.5989	225
		±3.04	±.008	±1.90	±.029	0.031	±2.9	±.0007	±1
	1400	12.52	0.215	18.70	0.748	0.775	13.9	0.9827	153
		±1.27	±.008	±.96	±.016	±.023	±.7	±.0014	±1
	1600-1	2.21	0.207	4.48	1.525	0.703	7.3	0.5371	260
		±.23	±.008	±.23	±.121	±.074	±.4	±.0010	±1
	1600-2	<0.91	n.d.	<0.37	n.d.	n.d.	2.0	0.2513	336
									±2
	Total	61.03	0.212	73.86	0.836	0.784	325.2	0.3203	288
		±3.59	±.005	±2.25	±.024	±.023	±7.7	±.0002	±1
Ni-Fe metal M									
(0.8713)	600	<0.199	n.d.	<0.005	n.d.	0.414	<0.074	n.d.	n.d.
						±.064			
	1600-1	50.67	0.251	8.403	0.874	0.881	21.71	1.653	7.224
		±3.71	±.005	±.618	±.005	±.009	±1.54	±.002	±.043
	1600-2	6.416	0.237	3.001	0.834	0.892	9.41	1.766	n.d.
		±.471	±.005	±.222	±.019	±.009	±.68	±.002	
	1600-3	1.232	0.226	1.253	0.800	0.891	4.98	1.681	n.d.
		±.090	±.004	±.093	±.022	±.010	±.36	±.002	
	1600-4	0.400	0.233	0.400	0.856	0.887	1.88	1.678	n.d.
		±.030	±.005	±.030	±.059	±.012	±.14	±.002	
	1600-5	0.337	0.228	0.197	0.846	0.880	0.87	1.653	n.d.
		±.025	±.005	±.015	±.115	±.017	±.06	±.004	
	Total	59.056	0.249	13.260	0.857	0.885	38.86	1.685	7.224
		±3.743	±.004	±.664	±.006	±.006	±1.73	±.001	±.043
Air[1]			1.399×10^{-6}		9.8	0.029		0.188	295.5
SW[2]			4.57×10^{-4}		13.8	0.0328		0.1786	
Q[3]			1.59×10^{-4}		10.7	0.0318		0.188	2.09
HL[4]			1.7×10^{-4}		8.5	0.036		0.277	<0.08
Cosmogenic[5]					0.853	0.914		1.5–1.75	
For TR and SC[6]					0.770	0.78			
For CR[7]					0.928	0.918			
For M[8]					0.842	0.886			

[1]Ozima and Podosek (2002), [2]Benkert et al. (1993), [3]Wieler et al. (1991), [4]Huss and Lewis (1994), [5]Scherer and Schults (2000), [6]Average of 1200 °C fraction for troilite and 1200 and 1400 °C fractions for schreibersite, [7]Average of 1200 °C fractions for chromite–2 and –3, [8]Total of 1600 °C fractions for Ni- Fe metal.

Table 2. Concentrations and isotopic compositions of Kr in inclusions and metal phase of the Saint-Aubin iron meteorite.

Sample weight (g)	Temp. (°C)	[^{84}Kr] (10^{-11} cm^{3}STP/g)	^{78}Kr	^{80}Kr	^{82}Kr	^{83}Kr	^{86}Kr
					^{84}Kr = 1		
Chromite							
CR2	600	0.74	0.00731	0.0419	0.185	0.182	0.284
(0.0887)		± .07	±.00133	±.0047	±.017	±.009	±.017
	800	1.16	0.00627	0.0349	0.193	0.191	0.296
		±.08	±.00123	±.0043	±.012	±.006	±.012
	1000	2.07	0.00640	0.0418	0.203	0.202	0.296
		±.13	±.00098	±.0024	±.007	±.005	±.007
	1200	2.10	0.00602	0.0386	0.202	0.199	0.304
		±.14	±.00063	±.0020	±.010	±.004	±.010
	1400	5.33	0.00487	0.0361	0.192	0.191	0.295
		±.35	±.00077	±.0026	±.007	±.006	±.007
	1600	1.77	0.00605	0.0382	0.202	0.192	0.319
		±.16	±.00237	±.0077	±.017	±.012	±.017
	Total	13.17	0.00571	0.0379	0.196	0.194	0.299
		± .44	±.00050	±.0016	±.004	±.003	±.004
CR3	800	5.37	n.d.	n.d.	0.199	0.246	0.314
(0.1345)		±.44			±.026	±.034	±.024
	1200	3.67	0.00586	0.0402	0.201	0.205	0.292
		±.27	±.00055	±.0043	±.020	±.022	±.007
	1600	1.04	0.00650	0.0338	0.212	0.195	0.295
		±.14	±.00104	±.0044	±.022	±.022	±.011
	1800-1	0.69	0.00372	0.0279	0.199	0.202	0.281
		±.12	±.00185	±.0056	±.024	±.024	±.014
	1800-2	0.23	<.03192	0.0300	0.249	0.192	0.274
		±.11		±.0141	±.049	±.044	±.053
	1800-3	<1.11	n.d.	n.d.	n.d.	n.d.	n.d.
	Total	11	0.00571	0.0371	0.202	0.224	0.302
		±.56	±.0048	±.0031	±.014	±.019	±.012
CR4	600	36.79	n.d.	n.d.	0.206	0.202	0.303
(0.1482)		±4.60			±.005	±.004	±.008
	1000	1.49	0.00805	0.0391	0.200	0.217	0.285
		±.17	±.00093	±.0018	±.005	±.004	±.009
	1400	2.19	n.d.	0.0384	0.201	0.200	0.298
		±.26		±.0018	±.004	±.005	±.006
	1800-1	1.49	0.00384	0.0383	0.219	0.199	0.316
		±.18	±.00109	±.0038	±.007	±.009	±.008
	1800-2	<1.08	n.d.	n.d.	n.d.	n.d.	n.d.
	1800-3	<1.07	n.d.	n.d.	n.d.	n.d.	n.d.
	1800-4	<0.36	n.d.	n.d.	n.d.	n.d.	n.d.
	Total	41.97	0.00595	0.0386	0.206	0.202	0.302
		±4.62	±.00072	±.0014	±.004	±.004	±.007
Troilite TR							
(0.1299)	600	0.68	0.00600	0.0386	0.210	0.188	0.304
		±.06	±.00159	±.0059	±.012	±.012	±.013
	800	0.41	0.00781	0.0455	0.178	0.213	0.349
		±.04	±.00325	±.0072	±.022	±.017	±.020
	1000	0.50	0.00703	0.0706	0.197	0.719	0.300
		±.04	±.00230	±.0069	±.015	±.033	±.022
	1200	0.25	0.01542	0.151	0.195	4.215	0.298
		±.03	±.00428	±.0174	±.029	±.394	±.041
	1400	0.15	<0.02931	0.1034	n.d.	2.701	0.164

Table 2. *Continued.* Concentrations and isotopic compositions of Kr in inclusions and metal phase of the Saint-Aubin iron meteorite.

Sample weight (g)	Temp. (°C)	[^{84}Kr] (10^{-11} cm^{3}STP/g)	^{78}Kr	^{80}Kr	^{82}Kr	^{83}Kr	^{86}Kr
					^{84}Kr = 1		
		±.03		±.0318		±.425	±.071
	1600	0.08	n.d.	0.0934	0.198	0.611	n.d.
		±.05		±.0559	±.108	±.251	
	Total	2.07	0.00796	0.0680	0.197	1.000	0.302
		±.11	±.00127	±.0048	±.009	±.058	±.011
Schreibersite SC							
(0.1214)	600	82.10	0.00599	0.0402	0.213	0.212	0.314
		±4.33	±.00009	±.0003	±.001	±.001	±.001
	800	29.06	0.00589	0.0405	0.204	0.207	0.302
		±1.59	±.00024	±.0005	±.002	±.002	±.003
	1000	121.25	0.00626	0.0412	0.214	0.21	0.309
		±6.41	±.00011	±.0003	±.001	±.001	±.001
	1200	49.03	0.00650	0.0410	0.213	0.211	0.312
		±2.60	±.00012	±.0004	±.002	±.001	±.001
	1400	5.19	0.00681	0.0403	0.203	0.209	0.298
		±.29	±.00036	±.0012	±.004	±.002	±.003
	1600-1	2.6	0.00575	0.0408	0.208	0.210	0.297
		±.17	±.00041	±.0010	±.004	±.004	±.005
	1600-2	0.50	0.00546	0.0479	0.197	0.224	0.289
		±.07	±.00161	±.0046	±.017	±.016	±.016
	Total	289.73	0.00619	0.0408	0.212	0.211	0.310
		±8.32	±.00006	±.0002	±.001	±.0005	±.001
Ni-Fe metal M							
(0.8713)	600	<0.086	n.d.	n.d.	n.d.	n.d.	n.d.
	1600-1	0.126	0.02636	0.0717	0.266	0.283	0.348
		±.015	±.00316	±.0038	±.011	±.012	±.016
	1600-2	<0.074	n.d.	n.d.	n.d.	n.d.	n.d.
	1600-3	<0.094	n.d.	n.d.	n.d.	n.d.	n.d.
	1600-4	<0.029	n.d.	n.d.	n.d.	n.d.	n.d.
	1600-5	<0.031	n.d.	n.d.	n.d.	n.d.	n.d.
	Total	0.126	0.02636	0.0717	0.266	0.283	0.348
		±.015	±.00316	±.0038	±.011	±.012	±.016
Air[1]			0.006087	0.0396	0.20217	0.20136	0.30524
SW[2]			0.006359	0.04075	0.20501	0.20276	0.30115
Q[3]			0.00621	0.03952	0.2015	0.2017	0.3099
HL[4]			0.0043	0.0308	0.16	0.1993	0.3603
Cosmogenic[5]			0.284	0.786	1.21	1.59	0.0241

[1]Ozima and Podosek (2002), [2]Pepin et al. (1995), [3]Wieler et al. (1992), [4]Huss and Lewis (1994), [5]Marti et al. (1966); Marti and Lugmair (1971).

atmosphere (Figs. 3–6). These data do not reveal the presence of cosmogenic Kr and Xe as it is obvious for metal. The fissiogenic Xe in chromite is slightly more abundant than the cosmogenic Xe. Moreover, the Xe data of the chromite samples (CR2 to 4) scatter in the ratio projections and also have variable concentrations (Fig. 5). The reason for the large variation is probably due to the fact that Saint-Aubin chromite is mostly pure Fe-chromite (Fehr and Carion 2004; Kurat et al. 2005), and because the target elements to produce the cosmogenic or the fissiogenic Kr and Xe (for example, Mo, Ru, Ir, Pt, Au, etc.) are present in very small amounts and are possibly inhomogeneously distributed.

Radiogenic and Epi-Thermal Neutron Capture Compositions in Troilite Inclusion

The ^{40}Ar/^{36}Ar ratios of troilite were higher than that of the air component at the gas extraction temperatures of 800 to 1200 °C as shown in Fig. 2. The 800 and 1000 °C fractions are

Table 3. Concentrations and isotopic compositions of Xe in inclusions and metal phase of the Saint Aubin iron meteorite.

Sample weight	Temp.	[^{132}Xe]	^{124}Xe	^{126}Xe	^{128}Xe	^{129}Xe	^{130}Xe	^{131}Xe	^{134}Xe	^{136}Xe
(g)	(°C)	(10^{-12} cm^3 STP/g)								
Chromite										
CR2	600	3.5	0.00370	n.d.	0.0715	1.02	0.140	0.791	0.378	0.404
(0.0887)		±.4	±.00137		±.0050	±.04	±.009	±.033	±.019	±.019
	800	1.0	n.d.	n.d.	0.0685	0.97	n.d.	0.831	0.369	0.390
		±.1			±.0153	±.08		±.062	±.067	±.063
	1000	3.4	0.00207	0.00158	0.0603	0.97	0.144	0.756	0.364	0.372
		±.4	±.00160	±.00122	±.0097	±.03	±.009	±.023	±.020	±.019
	1200	4.4	0.00612	0.00406	0.0622	0.98	0.138	0.778	0.345	0.361
		±.5	±.00163	±.00139	±.0072	±.05	±.011	±.030	±.023	±.022
	1400	17.2	0.00538	0.00305	0.0702	0.99	0.141	0.911	0.387	0.410
		±2.1	±.00125	±.00079	±.0069	±.02	±.007	±.021	±.010	±.010
	1600	1.2	n.d.	n.d.	0.0980	1.05	0.099	0.812	0.354	0.648
		±.3			±.0824	±.22	±.052	±.132	±.060	±.095
	Total	30.9	0.00489	0.00302	0.0692	0.99	0.139	0.855	0.375	0.407
		±2.3	±.00083	±.00062	±.0053	±.02	±.005	±.014	±.008	±.008
CR3	800	15.5	0.00434	0.00283	0.0702	1.02	0.152	0.806	0.383	0.307
(0.1345)		±2.5	±.00060	±.00088	±.0043	±.03	±.004	±.019	±.012	±.011
	1200	0.6	n.d.	n.d.	n.d.	n.d.	0.201	0.593	<3.636	0.755
		±.3					±.118	±.312		±.241
	1600	<3.2	n.d.	n.d.	n.d.	n.d.	n.d.	n.d.	n.d.	n.d.
	1800-1	<2.7	n.d.	n.d.	n.d.	n.d.	n.d.	n.d.	n.d.	n.d.
	1800-2	<3.2	n.d.	n.d.	n.d.	n.d.	n.d.	n.d.	n.d.	n.d.
	1800-3	<2.6	n.d.	n.d.	n.d.	n.d.	n.d.	n.d.	n.d.	n.d.
	Total	16.13	0.00434	0.00283	0.0702	1.02	0.154	0.798	0.383	0.324
		±2.56	±.00060	±.00088	±.0043	±.03	±.006	±.022	±.012	±.014
CR4	600	18.1	0.00458	0.00359	0.0735	0.957	0.145	0.797	0.445	0.323
(0.1482)		±1.9	±.00078	±.00091	±.0032	±.017	±.007	±.015	±.014	±.013
	1000	2.2	0.00882	0.00258	0.0745	1.067	0.142	0.806	0.365	0.327
		±.2	±.00219	±.00195	±.0055	±.042	±.010	±.030	±.024	±.024
	1400	2.7	0.00370	0.00521	0.0845	1.071	0.142	0.870	0.392	0.343
		±.3	±.00168	±.00169	±.0073	±.046	±.014	±.042	±.034	±.026
	1800-1	0.3	n.d.	n.d.	n.d.	n.d.	n.d.	1.293	0.439	n.d.
		±.2						±.485	±.215	
	1800-2	<2.3	n.d.	n.d.	n.d.	n.d.	n.d.	n.d.	n.d.	n.d.
	1800-3	<1.3	n.d.	n.d.	n.d.	n.d.	n.d.	n.d.	n.d.	n.d.
	1800-4	<0.6	n.d.	n.d.	n.d.	n.d.	n.d.	n.d.	n.d.	n.d.
	Total	23.3	0.00489	0.00368	0.00749	0.981	0.144	0.812	0.431	0.326
		±2.0	±.00068	±.00077	±.0027	±.015	±.006	±.014	±.012	±.011
Troilite TR										
(0.1299)	600	0.92	0.00424	n.d.	0.0737	1.09	0.137	0.851	0.356	0.366
		±.07	±.00406		±.0132	±.07	±.026	±.079	±.031	±.030
	800	0.47	0.01461	n.d.	0.1205	1.27	0.156	0.981	0.380	0.312
		±.05	±.00579		±.0235	±.17	±.052	±.144	±.049	±.065
	1000	0.86	n.d.	0.00756	0.0889	2.88	0.224	1.220	0.491	0.300
		±.06		±.00283	±.0162	±.17	±.030	±.071	±.035	±.034

Table 3. *Continued.* Concentrations and isotopic compositions of Xe in inclusions and metal phase of the Saint Aubin iron meteorite.

Sample weight (g)	Temp. (°C)	[^{132}Xe] (10^{-12} cm^3 STP/g)	^{124}Xe	^{126}Xe	^{128}Xe	^{129}Xe	^{130}Xe	^{131}Xe	^{134}Xe	^{136}Xe
			^{132}Xe = 1							
	1200	1.21 ±.09	0.00729 ±.00239	<0.00006	0.0882 ±.0110	5.82 ±.18	0.146 ±.025	1.794 ±.076	0.409 ±.034	0.251 ±.021
	1400	0.08 ±.06	n.d.	<0.02766	<0.5901	30.07 ±23.08	<1.457	7.035 ±5.039	1.155 ±.904	n.d.
	1600	0.41 ±.06	n.d.	n.d.	0.0799 ±.0367	1.73 ±.22	0.141 ±.122	1.163 ±.106	0.733 ±.136	0.391 ±.126
	Total	3.95 ±.16	0.00753 ±.00210	0.00756 ±.00283	0.0880 ±.00283	3.00 ±.46	0.162 ±.019	1.251 ±.107	0.436 ±.028	0.311 ±.020
Schreibersite SC (*0.1214)*	600	301 ±55	0.00336 ±.00014	0.00336 ±.00015	0.0711 ±.0013	0.99 ±.01	0.149 ±.002	0.795 ±.003	0.392 ±.002	0.332 ±.001
	800	124 ±23	0.00362 ±.00017	0.00338 ±.00017	0.0715 ±.0014	1.00 ±.01	0.145 ±.002	0.792 ±.004	0.390 ±.002	0.332 ±.002
	1000	553 ±101	0.00378 ±.00011	0.00345 ±.00012	0.0734 ±.0013	0.99 ±.01	0.153 ±.002	0.803 ±.003	0.404 ±.001	0.341 ±.002
	1200	266 ±49	0.00367 ±.00015	0.00342 ±.00017	0.0709 ±.0014	1.00 ±.01	0.151 ±.002	0.790 ±.004	0.387 0.002	0.332 ±.002
	1400	26 ±55	0.00414 ±.00050	0.00397 ±.00042	0.0720 ±.0027	1.00 ±.01	0.151 ±.004	0.814 ±.010	0.390 ±.004	0.334 ±.006
	1600-1	13 ±23	0.00277 ±.00058	0.00298 ±.00057	0.0659 ±.0029	0.99 ±.01	0.150 ±.005	0.778 ±.016	0.376 ±.009	0.327 ±.006
	1600-2	1.2 ±0.2	<0.00549	0.00994 ±.00294	0.0632 ±.0188	0.92 ±.10	0.158 ±.023	0.686 ±.044	0.392 ±.034	0.284 ±.048
	Total	1283 ±127	0.00364 ±.00007	0.00343 ±.00007	0.0721 ±.0007	0.99 ±.00	0.151 ±.001	0.797 ±.002	0.396 ±.001	0.336 ±.001
Ni-Fe metal M *(0.8713)*	600	0.055 ±.012	n.d.	n.d.	n.d.	1.07 ±.23	0.134 ±.053	1.268 ±.274	0.813 ±.156	0.416 ±.112
	1600-1	0.269 ±.031	n.d.	0.00261 ±.00250	0.0860 ±.0104	1.10 ±.08	±.126 ±.018	0.768 ±.056	0.358 ±.030	0.355 ±.035
	1600-2	<0.065	n.d.	n.d.	n.d.	n.d.	n.d.	n.d.	n.d.	n.d.
	1600-3	<0.102	n.d.	n.d.	n.d.	n.d.	n.d.	n.d.	n.d.	n.d.
	1600-4	<0.035	n.d.	n.d.	n.d.	n.d.	n.d.	n.d.	n.d.	n.d.
	1600-5	<0.069	n.d.	n.d.	n.d.	n.d.	n.d.	n.d.	n.d.	n.d.
	Total	0.324 ±.033	n.d.	0.00261 ±.00250	0.0860 ±.0104	1.10 ±.08	0.128 ±.018	0.852 ±.065	0.435 ±.036	0.365 ±.034
Air[1]			0.003537	0.0033	0.07136	0.9832	0.15136	0.789	0.3879	0.3297
SW[2]					0.0849	1.054	0.1656	0.8255	0.366	0.297
Q[3]			0.00464	0.00413	0.0826	1.036	0.1624	0.8174	0.3801	0.3181
HL[3]			0.00842	0.00569	0.0905	1.056	0.1544	0.8442	0.6361	0.7
El Taco Xe[4]			0.00394	0.00358	0.0748	1.156	0.1542	0.7930	0.3843	0.3222
(Modified)[5]			0.00387	0.00354			0.1537	0.7916	0.382	0.3200
Cosmogenic[6]			4.9	5	5.6	6.1	0.155	6.7	0.4	

[1]Ozima and Podosek (2002), [2]Wieler and Baur (1994), [3]Huss and Lewis (1994), [4]Mathew and Begemann (1995), [5]Maruoka (1999), [6]Munk (1967).

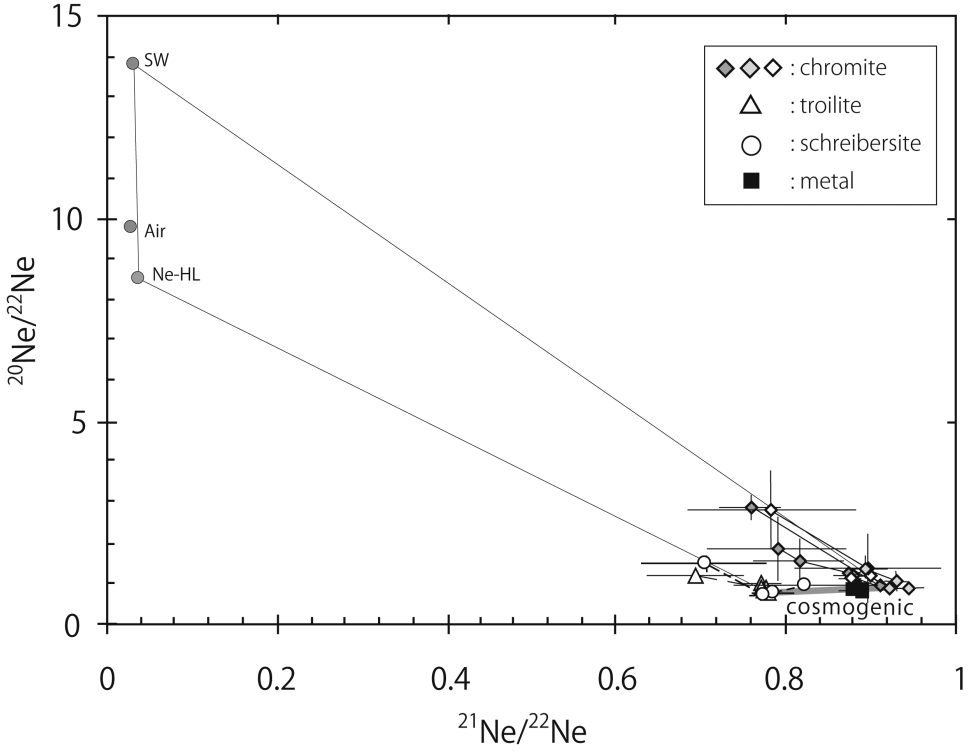

Fig. 1. Ne three-isotope plot of $^{20}Ne/^{22}Ne$ versus $^{21}Ne/^{22}Ne$ ratios. "SW" and "Air" are solar wind (Benkert et al. 1993) and terrestrial atmospheric components (Ozima and Podosek 2002), respectively. The cosmogenic values were taken from Scherer and Schultz (2000).

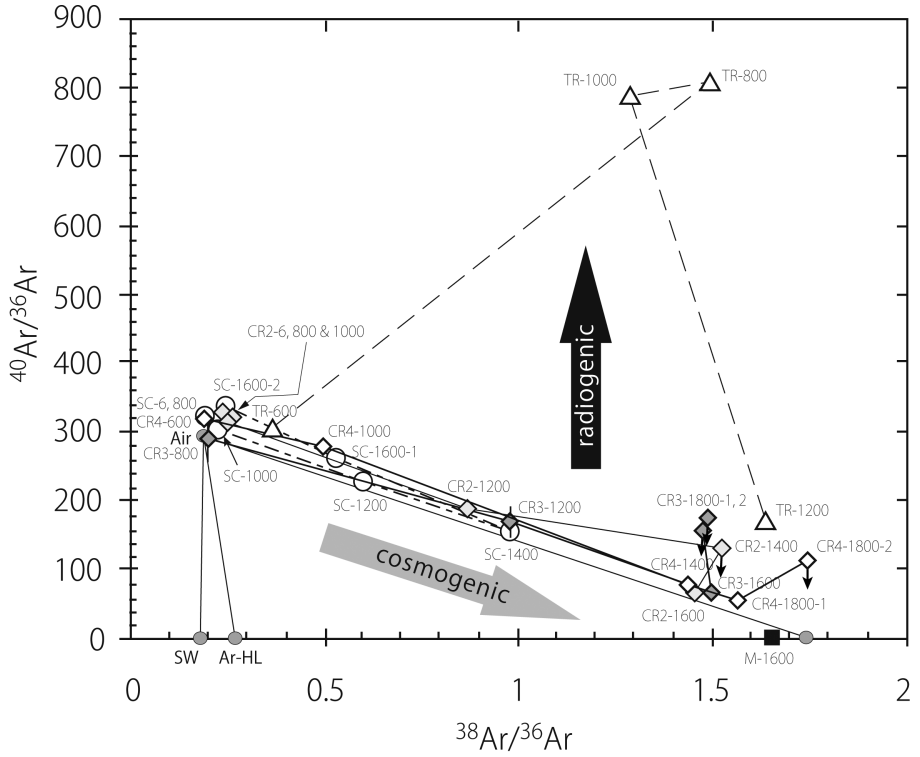

Fig. 2. Ar three-isotope plot of $^{40}Ar/^{36}Ar$ versus $^{38}Ar/^{36}Ar$ ratios. The numerical values are the release temperature (°C) of stepwise heating. The literature values were taken from Ozima and Podosek (2002) for terrestrial air (Air), Benkert et al. (1993) for solar wind (SW), Huss and Lewis (1994) for Ar-HL, and Scherer and Schultz (2000) for the cosmogenic component. The data points from troilite are located above the mixing line between Air and cosmogenic component due to the presence of radiogenic ^{40}Ar.

Table 4. The production rates and the cosmic-ray exposure ages for ^{3}He of the Saint-Aubin iron meteorite.

Sample		P'_3	P_3	T'_3[1]	T_3[1]
		10^{-10} cm^3 STP/g per Ma		Ma	
Chromite	(CR3)	131	132	15.9 ± 0.4	15.9 ± 0.4
	(CR4)			15.8 ± 0.9	15.7 ± 0.9
				15.9 ± 0.5	15.8 ± 0.5
Troilite	(TR)	140	133	11.8 ± 0.5	13.1 ± 0.6
Schreibersite	(SC)	148	141	8.7 ± 0.5	9.2 ± 0.6
Metal	(M)	117	116	12.6 ± 0.8	12.6 ± 0.8

[1]T'_3 is the exposure age using the production rate P'_3, and T_3 is the exposure age using the production rate using P_3.

especially rich in ^{40}Ar with ^{40}Ar/^{36}Ar ratios of 812 ± 15 for 800 °C and 787 ± 14 for 1000 °C. The excess of ^{40}Ar is possibly radiogenic, produced by the radioactive decay of ^{40}K. However, trace element analyses of troilite (Kurat, unpublished data) show very low K contents, consequently we have to assume that it contains some K-rich inclusions. The low decomposition temperature of this phase could indicate the presence of a K sulfide. Under reducing conditions, K becomes chalcophile and forms sulfides. These could co-precipitate with troilite, get trapped, and be isolated from later oxidizing conditions. The excess for the radiogenic ^{40}Ar* in the bulk troilite is calculated to be $(7.82 \pm 0.23) \times 10^{-7}$ cm^{3}STP/g. Assuming that the radiogenic ^{40}Ar is the decay product from ^{40}K in troilite over the past 4.55 billion years and that the produced ^{40}Ar remained in a closed system, we can estimate that the K content in troilite was 9.7 ppm. The amount found by SIMS is 2.47 and 1.5 ± 0.03 ppm for 2 separate analysis points (Kurat, unpublished data). The data indicate the inhomogeneous presence of a phase—apparently, we did not hit proper K-rich pockets, which must contain more than 10 ppm.

The isotopic composition of Kr in troilite is shown in Fig. 3. The excesses of ^{80}Kr and ^{83}Kr in the troilite are distinct. The excess of ^{80}Kr in Fig. 3a was produced by neutron capture on Br or by proton capture on Se. Excess of ^{83}Kr relative to the terrestrial atmosphere is also indicated in troilite (Fig. 3b) and is $1.65 \pm 0.15 \times 10^{-11}$ cm^{3}STP/g. The excess can be explained by the neutron capture on ^{82}Se. Such excess of ^{83}Kr in troilite has previously been found in both magmatic and non-magmatic iron meteorites (Clarke and Thode 1964; Alexander and Manuel 1968; Alexander et al. 1968; Haag and Kirsten 1975; Murty and Marti 1987). Therefore, it is plausible that the excess of ^{80}Kr in Saint-Aubin troilite was also produced by the (p,n) reaction on Se. Such excess Kr has also been reported from the Great Namaqualand (IVA) iron (Alexander et al. 1968). In Fig. 3a, the data of Saint-Aubin, particularly that of the 800 °C fraction, are slightly shifted from the air—Se(p,n) reaction (^{80}Kr/^{82}Kr ~ 5; Murty and Marti 1987) mixing line to the lower side of ^{82}Kr/^{84}Kr ratio. We supposed that this shift is produced by fissiogenic ^{84}Kr. This is because the 800 °C fraction of troilite shows a low ^{84}Kr/^{86}Kr ratio of 2.86 ± 0.17, which may be due to the fission of uranium.

Troilite is also enriched in ^{124}Xe, ^{126}Xe, ^{128}Xe, ^{129}Xe, and ^{131}Xe relative to the terrestrial atmosphere, in addition to the excess of ^{134}Xe. The ^{124}Xe, ^{126}Xe, and ^{128}Xe enrichment indicate the presence of cosmogenic products. The excesses of ^{129}Xe and ^{131}Xe in troilite are shown in Fig. 4. The trend of the excesses in Saint-Aubin troilite is similar to the trend of Great Namaqualand troilite (Alexander et al. 1968), Cape York troilite (Murty and Marti 1987), and Bohumilitz metal (Maruoka et al. 2001). It is likely that the excesses of these fractions are due to epi-thermal neutron capture on ^{128}Te and ^{130}Te (E > 0.4 eV; ^{129}Xe/^{131}Xe = 3.9 ± 0.5; Browne and Berman 1973). The ^{129}Xe is also produced by the ^{129}I radioactive decay (e.g., graphite of Canyon Diablo; Alexander and Manuel 1967, 1968; Matsuda et al. 2005), and the 1200 °C fraction slightly below the line of the epi-thermal neutron capture on Te may be due to radiogenic ^{129}Xe (Fig. 4). The 600, 800, and 1600 °C fractions are off the mixing line between the cosmogenic and the air components. They are enriched in the cosmogenic component or the products of thermal neutron capture with E < 0.4 eV on Te (^{129}Xe/^{131}Xe = 0.68; Browne and Berman 1973) in addition to that of epi-thermal neutron capture reaction with E > 0.4 eV, compared to the 1000 and 1200 °C fractions.

Primordial HL Component in Schreibersite

The ^{132}Xe concentration in schreibersite is much the same as that of graphite from the Canyon Diablo iron (Alexander and Manuel 1968; Matsuda et al. 2005) and higher than that of the schreibersite in Acuña by about two orders of magnitude (Matsuda et al. 1996). The concentration in schreibersite is higher than that in other phases. Thus we could determine the Xe isotopic ratios in schreibersite with better accuracy than that of other phases (Table 3). The 600, 800, and 1200 °C fractions of schreibersite have a ^{129}Xe/^{132}Xe ratios higher than that of the terrestrial atmosphere, but the ^{129}Xe excesses are not so large or different from that of troilite. The Xe isotopic ratios of those temperature fractions do not show the El Taco Xe or Xe-Q components (Figs. 5 and 6). The 1600 °C fraction of schreibersite overlaps the terrestrial atmosphere within the error. The 1000 and 1400 °C fractions show the influence of the cosmogenic component in Fig. 4 and of the thermal neutron capture on Te or the cosmogenic in Fig. 3.

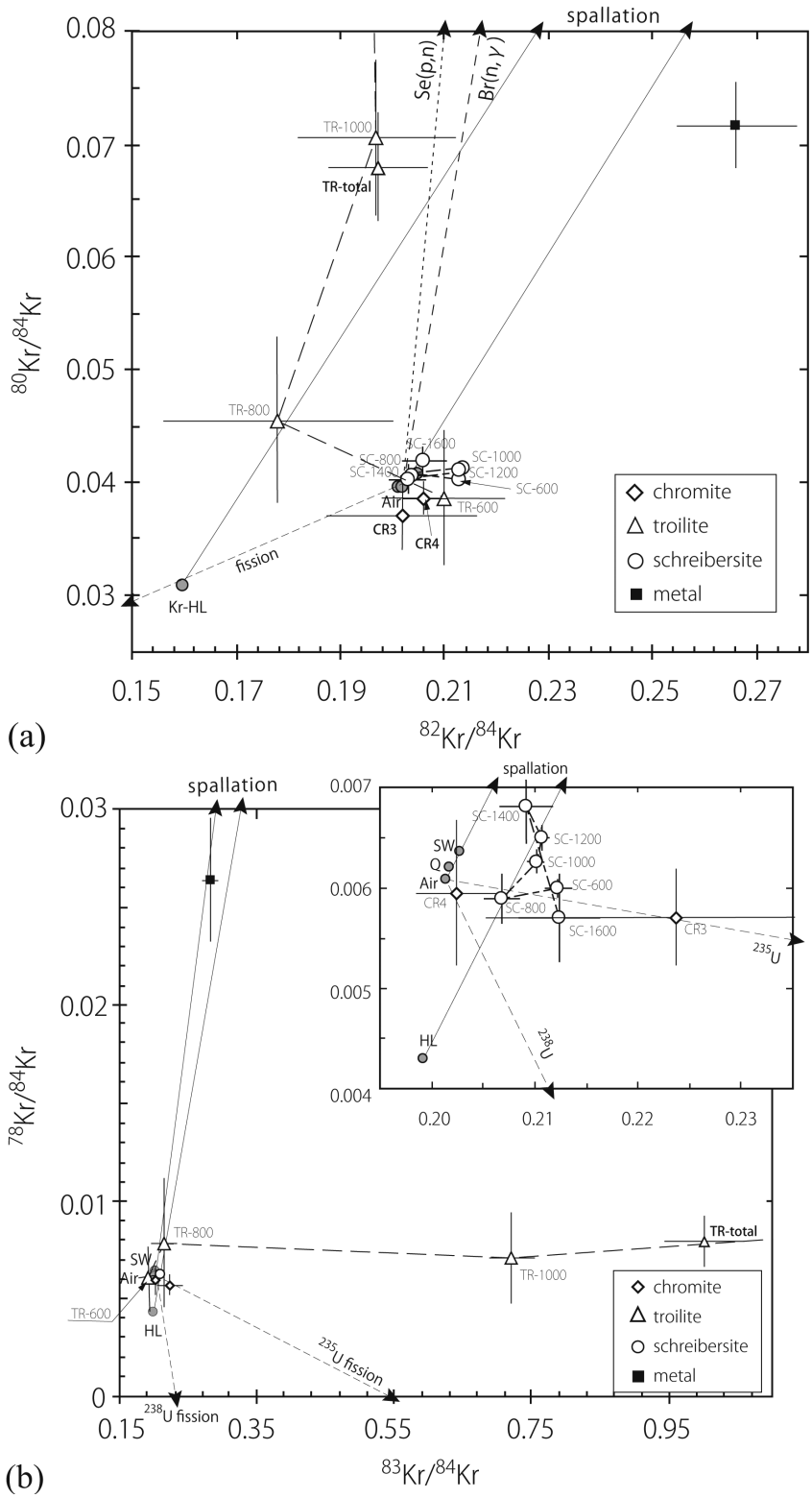

Fig. 3. The diagrams of Kr isotopic ratios. The numerical values are the release temperature (°C) of stepwise heating. The solid lines show the direction of the effect by spallogenic Kr (Marti et al. 1966; Marti and Lugmair 1971). The data of Air (Ozima and Podosek 2002), SW (Pepin et al. 1995), Q (Wieler et al. 1992), and HL (Huss and Lewis 1994) components are shown in Table 2. a) The diagram of $^{80}Kr/^{84}Kr$ versus $^{82}Kr/^{84}Kr$ ratios. The dashed arrow represents the direction to the Br (n, γ) reaction ($^{80}Kr/^{82}Kr \approx 3$), and the dotted arrow to the Se (p, n) reaction ($^{80}Kr/^{82}Kr \approx 5$) (Murty and Marti 1987). b) The diagram of $^{78}Kr/^{84}Kr$ versus $^{83}Kr/^{84}Kr$ ratios. The upper diagram shows enlarged area for the data from schreibersite.

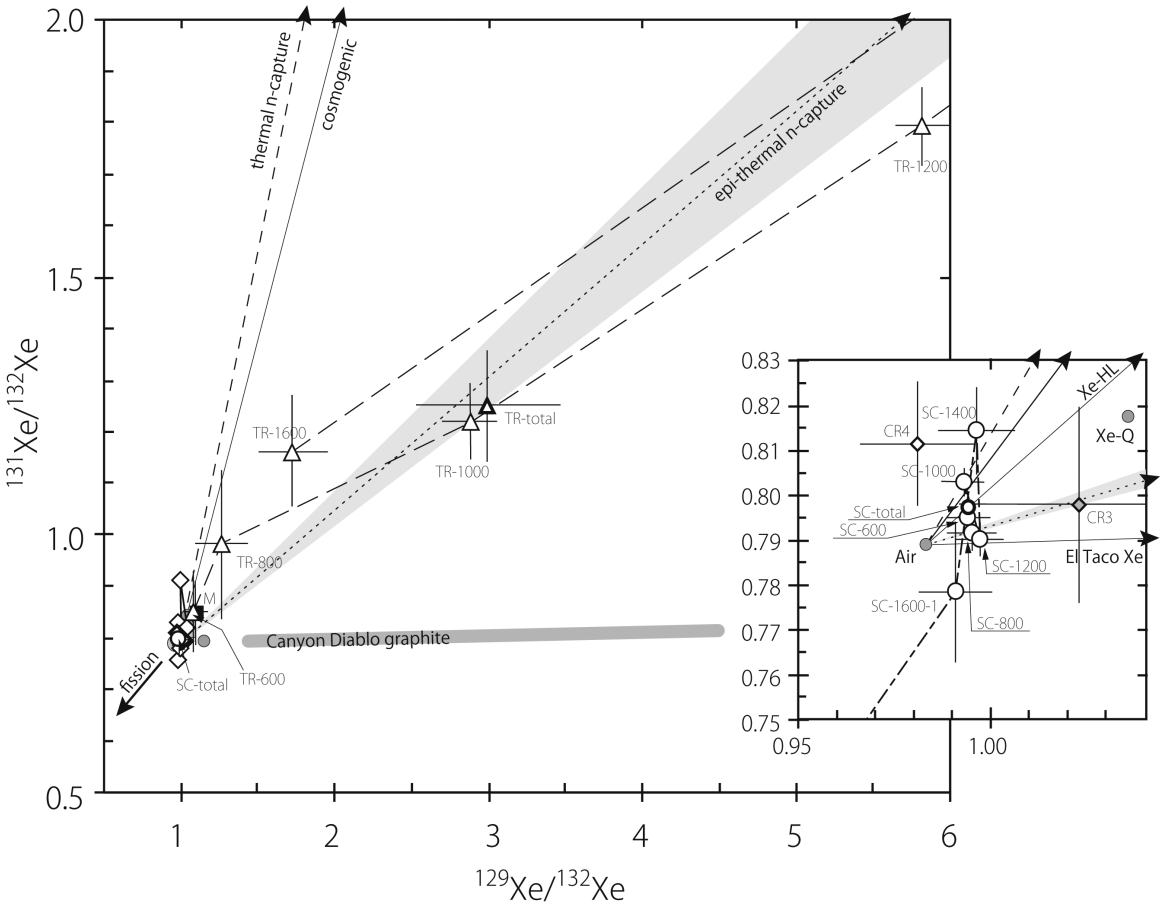

Fig. 4. The diagram of $^{131}Xe/^{132}Xe$ versus $^{129}Xe/^{132}Xe$ ratios. The numerical values are the release temperature (°C) of stepwise heating. The solid lines show the direction of the effect by spallogenic Xe (Munk 1967). The dashed and dotted lines represent the directions to thermal neutron capture (E < 0.4 eV) and epi-thermal neutron capture (E > 0.4 eV) reactions on Te, respectively (Browne and Berman 1973). The horizontal grayish bar is the area of distribution for the 600 to 1800 °C fractions of the Canyon Diablo graphite (Matsuda et al. 2005). The diagram at right shows the enlarged area of the data from the schreibersite.

In the diagrams of $^{130}Xe/^{132}Xe$ versus $^{136}Xe/^{132}Xe$ (Fig. 6) and $^{124}Xe/^{132}Xe$ versus $^{136}Xe/^{132}Xe$ (Fig. 7), it seems that there is Xe-HL present in the 1000 °C fraction. This temperature is just the release temperature of Xe-HL (Anders 1988). The Xe-HL component comprises about 5% of the 1000 °C fraction of schreibersite and that corresponds to 2.3×10^{-13} cm^3STP/g for ^{124}Xe. Thus, the Xe components in the schreibersite of Saint-Aubin are very different from those of the Acuña (IIIAB) iron. The other primordial Xe-Q and El Taco Xe components in the graphite of non-magmatic Canyon Diablo (IAB) are not observed in Saint-Aubin (Figs. 6 and 7). If it is true, it is likely that the primordial noble gases were totally released from most minerals in a heating process.

We can envision three possibilities for the presence of the Xe-HL component in the schreibersite of the Saint-Aubin (UNGR) iron meteorite. First, presolar diamond as the carrier of the HL component partly survived the melting in the core of the Saint-Aubin parent body. The presolar grains would have to survive very high temperatures and be captured by the crystal seed of schreibersite. Secondly, the parent body or the meteoroid of Saint-Aubin collided with a chondritic body. The presolar diamond got mixed into the Saint-Aubin schreibersite during re-assembly and iron formation. This could be the better process than the former because shock alteration has been shown to lead to preferential loss of the Q component relative to HL component (Nakamura et al. 1997), and because we do not observe the Q component in schreibersite. However, if the Xe-HL component in Saint-Aubin was admixed by collision with a chondritic body, the Saint-Aubin iron meteorite may hold silicate inclusions and should contain also a chondritic noble gas component, which is not the case. Therefore, we have to consider a third possible scenario: collection of presolar diamonds by the growing schreibersite in the solar nebula. Schreibersite, like chromite and troilite (and the phosphates present in Saint-Aubin) were formed before the metal collected and preserved them. This view is supported by the finding of excess ^{53}Cr in Saint-Aubin phosphates (Kurat et al. 2005). As chromite and phosphates clearly are secondary phases that formed by oxidation of

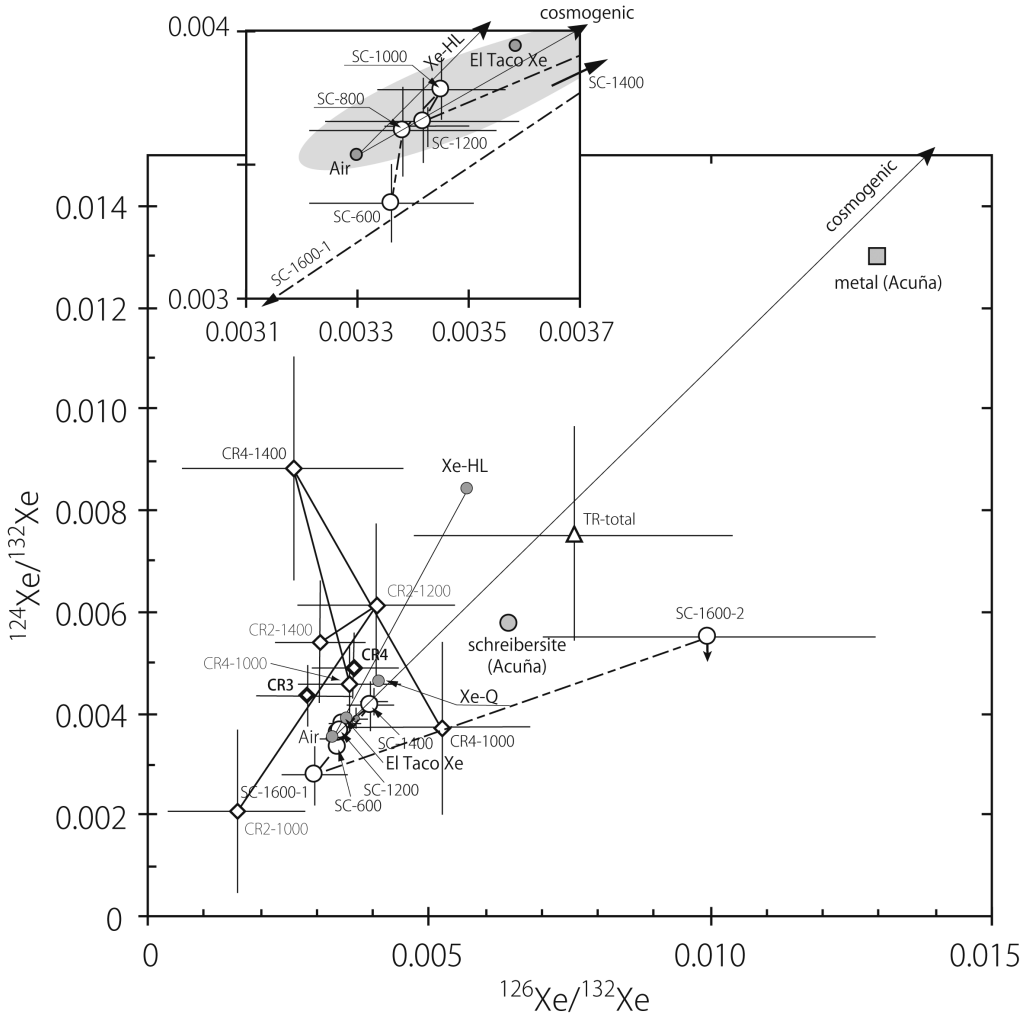

Fig. 5. The diagram of $^{124}Xe/^{132}Xe$ versus $^{126}Xe/^{132}Xe$ ratios. The numerical values are the release temperature of stepwise heating. The solid line shows the directions between Air to cosmogenic component or to Xe-HL component. The data of Air, cosmogenic, Xe-HL, and Q are given in Table 3. The data of El Taco Xe and Acuña are from Mathew and Begemann (1995) and Matsuda et al. (1996), respectively. The upper diagram shows the enlarged area for the data of the schreibersite.

reduced precursors, these phases should be very poor in primordial gases. However, the phosphates do keep a memory of very early times in the solar nebula. Consequently, schreibersite appears to be a primary solar nebula phase (e.g., Kurat et al. 2002).

However, it is also possible to interpret the deviation of $^{136}Xe/^{132}Xe$ as a mixture of fission and spallation effects. In Fig. 7, the schreibersite data point of the 1000 °C fraction is above the fission line, but if spallation effect is added this data point goes to the upper direction. In fact, schreibersites in iron meteorites contain several ppm of trace elements such as Ir, Pt, and Au and their concentrations are correlated with grain size (Jochum et al. 1980). As shown later, Kr data also show the contributions of spallation and fission components. Thus, further study is necessary to confirm the presence of the Xe-HL component.

The light noble gases in schreibersite appear to be a mixture between the cosmogenic component and the terrestrial air, as discussed above, and are dominated by the cosmogenic component. The primordial HL component could not be observed in the light noble gases.

Krypton isotopic composition in schreibersite of the Saint-Aubin (UNGR) iron meteorite shows a small difference to that in the Acuña (IIIAB) iron (Matsuda et al. 1996). The temperature fractions of Saint-Aubin schreibersite roughly plot along the line from the Kr-HL component to the products of the cosmic-ray exposure in the three-isotope diagram for $^{78}Kr/^{84}Kr$ versus $^{83}Kr/^{84}Kr$ (Fig. 3b). Some data are situated on the right side of the HL-cosmogenic Kr mixing line. The shift has been observed in troilite and is possible due to the presence of fission products of uranium. Such a contribution for the Kr-HL component could not be observed in the $^{80}Kr/^{84}Kr$ versus $^{82}Kr/^{84}Kr$ diagram (Fig. 3a). The 600, 1000, and 1200 °C fractions shift to the trend of ^{235}U fission. Therefore, krypton isotopes in schreibersite appear to have contributions from spallation and ^{235}U fission. There is no large effect of

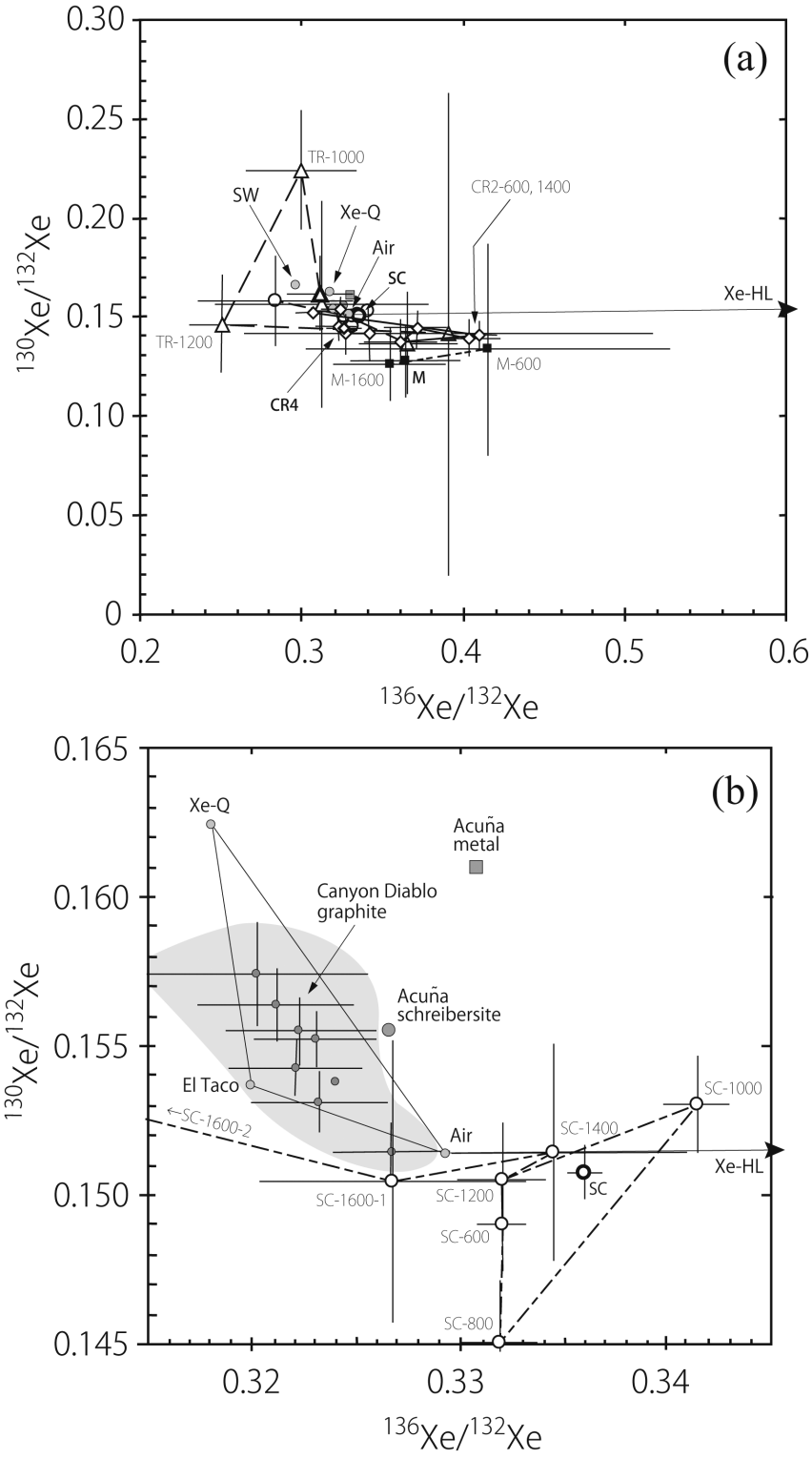

Fig. 6. a) Three-isotope plot of $^{136}Xe/^{132}Xe$ versus $^{130}Xe/^{132}Xe$ ratios for all samples. The numerical values are the release temperature of stepwise heating. The data of Air, cosmogenic, Xe-HL, and Q are given in Table 3. b) Enlarged diagram of the data for the schreibersite and the primordial components. Grey area is the projection area for the Canyon Diablo graphite data (Matsuda et al. 2005). The data of El Taco Xe and Acuña were taken from Mathew and Begemann (1995) and Matsuda et al. (1996), respectively.

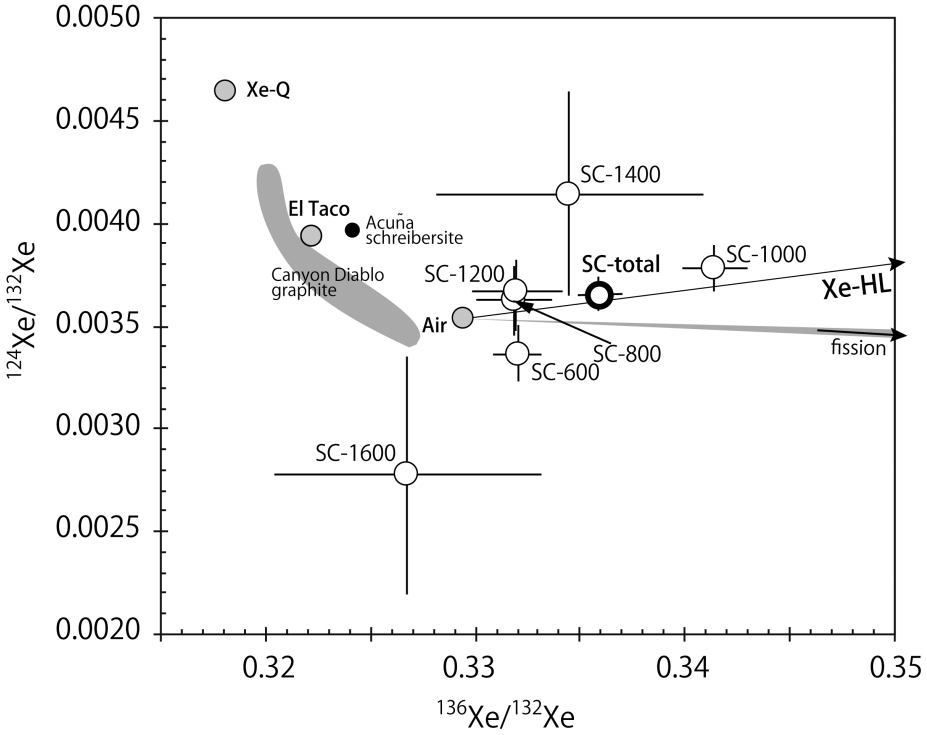

Fig. 7. The diagram of $^{124}Xe/^{132}Xe$ versus $^{136}Xe/^{132}Xe$ ratios of schreibersite. The numerical values are the release temperature of stepwise heating. The solid arrow represents the direction from Air to Xe-HL, and the shaded arrow shows the effect of fissiogenic Xe. The data of Air, cosmogenic, Xe-HL, and Q are given in Table 3. The data of El Taco Xe and Acuña were taken from Mathew and Begemann (1995) and Matsuda et al. (1996), respectively.

fission in Fig. 3a because the production rate for ^{84}Kr by fission is low.

CONCLUSIONS

We analyzed the noble gas concentrations and isotopic ratios in the inclusions (chromite, troilite, and schreibersite) and the Ni-Fe metal of the Saint-Aubin (UNGR) iron meteorite using the stepwise heating technique to separate the noble gas components in the samples. We have obtained several important results from this study:

(1) The cosmogenic components are predominant in the light noble gases in all phases. The noble gas concentrations in the metal are among the lowest encountered so far in an iron meteorite and $^{4}He/^{21}Ne$ is as high as 503. The Saint-Aubin iron meteorite is supposed to have had a relatively large pre-atmospheric size, comparable to that of Canyon Diablo, Odessa, and Acuña.

(2) The estimated exposure ages from ^{3}He are 9–16 Ma, that is about an order of magnitude younger than those of common iron meteorites.

(3) Troilite of the Saint-Aubin iron meteorite contains excesses of $^{80, 82}Kr$ due to the neutron capture by Se and $^{129, 131}Xe$ from the epi-thermal neutron capture (E > 0.4 eV) by Te. The troilite is also enriched in radiogenic ^{40}Ar, possibly produced by the ^{40}K radioactive decay. The concentration of radiogenic ^{40}Ar is $7.82 \pm 0.23 \times 10^{-7}$ cm^3STP/g. The K content in troilite must be about 10 ppm, which is at odds with SIMS analytical data. Potassium probably has a solid carrier of its own (possibly a sulfide).

(4) Although it is not finally confirmed, it is likely that the 1000 °C fraction of schreibersite contains about 5% of the Xe-HL component, in spite of the fact that Saint-Aubin is classified as a magmatic iron meteorite (Ulff-Møller 1998; Fehr and Carion 2004). If it is true, then the primordial noble gases must have been totally released from the melted matter during a magmatic process. It is suggested that the Saint-Aubin iron meteorite experienced formation conditions different from those of common magmatic iron meteorites. However, the presolar diamond (host phase of Xe-HL) indicates access of the growing schreibersite to presolar diamond and, consequently, it probably records the growth of schreibersite in the solar nebula. However, further studies are necessary to confirm the presence of Xe-HL in this meteorite.

Acknowledgments–This study is partially supported by a Research Fellowship of the Japan Society for the Promotion of Science for Young Scientists. Financial support was received in Austria from FWF, the Academy of Sciences and the Freunde des Naturhistorischen Museums in Wien. We also thank Dr. Heck and an anonymous reviewer for their critical comments.

Editorial Handling—Dr. Timothy Swindle

REFERENCES

Alexander E. C. Jr. and Manuel O. K. 1967. Isotopic anomalies of krypton and xenon in Canyon Diablo graphite. *Earth and Planetary Science Letters* 2:220–224.

Alexander E. C., Jr. and Manuel O. K. 1968. Xenon in the inclusions of Canyon Diablo and Toluca iron meteorites. *Earth and Planetary Science Letters* 4:113–117.

Alexander E. C., Jr., Bennet J. H., and Manuel O. K. 1968. On noble gas anomalies in the Great Namaqualand troilite. *Zeitschrift für Naturforschung* 23a:1266–1271.

Ammon K. and Leya I. 2007. The influence of mineral inclusions on the production rates of cosmogenic nuclides in Grant (IIIAB) and Carbo (IID) (abstract). *Meteoritics & Planetary Science* 42: A13.

Ammon K., Masarik J., and Leya I. 2007. The relevance of noble gases in iron meteorites (abstract #1275). 38th Lunar and Planetary Science Conference. CD-ROM.

Anders E. 1988. Circumstellar material in meteorites: Noble gases, carbon and nitrogen. In *Meteorite and the early solar system*, edited by Kerridge J. F. and Matthews M. S. Tucson: The University of Arizona Press. pp. 927–955.

Benkert J. P., Baur H., Signer P., and Wieler R. 1993. He, Ne, and Ar from the solar wind and solar energetic particles in lunar ilmenites and pyroxenes. *Journal of Geophysical Research* 98: 13,147–13,162.

Bogard D. D., Huneke J. C., Burnett D. S., and Wasserburg G. J. 1971. Xe and Kr analyses of silicate inclusions from iron meteorites. *Geochimica et Cosmochimica Acta* 35:1231–1254.

Browne J. C. and Berman B. L. 1973. Neutron capture cross sections for ^{128}Te and ^{130}Te and the xenon anomaly in old tellurium ores. *Physical Review* C8:2405–2411.

Bunch T. E., Keil K., and Huss G. I. 1972. The Landes meteorite. *Meteoritics* 7:31–38.

Clarke W. B. and Thode H. G. 1964. The isotopic composition of krypton in meteorites. *Journal of Geophysical Research* 69: 3673–3679.

Dransart E. and Baron M. 2003. Saint-Aubin: The new French meteorite. *Meteorite!* 9:40–42.

Eugster O. and Michel Th. 1995. Common asteroid break-up events of eucrites, diogenites, and howardites and cosmic-ray production rates for noble gases in achondrites. *Geochimica et Cosmochimica Acta* 59:177–199.

Fehr K. T. and Carion A. 2004. Unusual large chromite crystals in the Saint-Aubin iron meteorite. *Meteoritics & Planetary Science* 39: A139–A141.

Gros J. and Anders E. 1977. Gas-rich minerals in the Allende meteorite: Attempted chemical characterization. *Earth and Planetary Science Letters* 33:401–406.

Haag H. and Kirsten T. 1975. Neutron capture profiles in the Mundrabilla iron meteorite. *Meteoritics* 10:408–409.

Heck Ph. R., Schmitz B., Baur H., Halliday A. N., and Wieler R. 2004. Fast delivery of meteorites to Earth after a major asteroid collision. *Nature* 430:323–325.

Heck Ph. R., Schmitz B., Baur H., and Wieler R. 2005. Determination of production rates of cosmogenic He and Ne in meteoritic chromite grains (abstract #1712). 36th Lunar and Planetary Science Conference. CD-ROM.

Huss G. R. and Lewis R. S. 1994. Noble gases in presolar diamonds I: Three distinct components and their implications for diamond origins. *Meteoritics* 29:791–810.

Jentsch O. and Schultz L. 1996. Cosmogenic noble gases in silicate inclusions of iron meteorites: Effects of bulk composition on elemental production rates. *Journal of the Royal Society of Western Australia* 79:67–71.

Jochum K. P., Seufert M., and Begemann F. 1979. On the distribution of major and trace elements between metal and phosphide phases of some iron meteorites. *Zeitschrift für Naturforschung* 35a:57–63.

Kleine T., Mezger K., Palme H., Scherer E., and Münker C. 2005. Early core formation in asteroids and late accretion of chondrite parent bodies: Evidence from ^{182}Hf-^{182}W in CAIs, metal-rich chondrites, and iron meteorites. *Geochimica et Cosmochimica Acta* 24:5805–5818.

Koblitz J. 2003. MetBase. CD-ROM.

Kurat G. 2003. Why iron meteorites cannot be samples of planetesimal smelting (abstract). Symposium, Evolution of Solar System Materials: A New Perspective from Antarctic Meteorites, Tokyo: National Institute of Polar Research. pp. 65–66.

Kurat G., Sylvester P., Kong P., and Brandstätter F. 2000. Heterogeneous and fractionated metal in Canyon Diablo (IA) graphite—metal rock (abstract #1666). 31st Lunar and Planetary Science Conference. CD-ROM.

Kurat G., Varela M. E., Ametrano S. J., and Brandstätter F. 2002. Major, minor and trace element abundances in metal and schreibersite of the San Juan mass of Campo del Cielo (IAB) (abstract #1781). 33rd Lunar and Planetary Science Conference. CD-ROM.

Kurat G., Zinner E., and Varela M. E. 2005. Trace element abundances in St. Aubin (UNGR iron) giant chromite and associated phases (abstract). *Meteoritics & Planetary Science* 40:A88.

Lewis R. S., Gros J., and Anders E. 1977. Isotopic anomalies of noble gases in meteorites and their origins 2. Separated minerals from Allende. *Journal of Geophysical Research* 82:779–792.

Levsky L. K. and Komarov A. N. 1975. He, Ne and Ar isotopes in inclusions of some iron meteorites. *Geochimica et Cosmochimica Acta* 39:275–284.

Leya I., Begemann F., Weber H. W., Wieler R., and Michel R. 2004. Simulation of the interaction of galactic cosmic ray protons with meteoroids: On the production of ^{3}He and light noble gas isotopes in isotropically irradiated thick gabbro and iron targets. *Meteoritics & Planetary Science* 39:367–386.

Marti K. and Lugmair G. W. 1971. Kr^{81}-Kr and K-Ar^{40} ages, cosmic-ray spallation products, and neutron effects in lunar samples from Oceanus Procellarum. Proceedings, 2nd Lunar Science Conference. pp. 1591–1605.

Marti K., Eberhardt P., and Geiss J. 1966. Spallation, fission, and neutron capture anomalies in meteoritic krypton and xenon. *Zeitschrift für Naturforschung* 21a:398–413.

Maruoka T., Matsuda J., and Kurat G. 2001. Abundance and isotopic composition of noble gases in metal and graphite of the Bohumilitz IAB iron meteorite. *Meteoritics & Planetary Science* 36:597–609.

Mathew K. J. and Begemann F. 1995. Isotopic composition of xenon and krypton in silicate-graphite inclusions of the El Taco, Campo del Cielo, IAB iron meteorite. *Geochimica et Cosmochimica Acta* 59:4729–4746.

Matsuda J., Matsubara K., Yajima H., and Yamamoto K. 1989. Anomalous Ne enrichment in obsidians and Darwin glass: Diffusion of noble gases in silica-rich glasses. *Geochimica et Cosmochimica Acta* 53:3025–3033.

Matsuda J., Nagao K., and Kurat G. 1996. Noble gases in metal and schreibersite of the Acuña (IIIAB) iron meteorite. *Meteoritics & Planetary Science* 31:227–233.

Matsuda J., Matsumoto T., Sumino H., Nagao K., Yamamoto J., Miura Y., Kaneoka I., Takahata N., and Sano Y. 2002. The ^{3}He/^{4}He ratio of the new internal He Standard of Japan (HESJ). *Geochemical Journal* 36:191–195.

Matsuda J., Namba M., Maruoka T., Matsumoto T., and Kurat G. 2005. Primordial noble gases in a graphite-metal inclusion from the Canyon Diablo IAB iron meteorite and their implications. *Meteoritics & Planetary Science* 40:431–443.

Murty S. V. S. and Marti K. 1987. Nucleogenic noble gas components in the Cape York iron meteorite. G*eochimica et Cosmochimica Acta* 51:163–172.

Munk M. N. 1967. Spallation neon, argon, krypton, and xenon in an iron meteorite. *Earth and Planetary Science Letters* 2:301–309.

Nakamura T., Zolensky M. E., Hörz F., Takaoka N., and Nagao K. 1997. Impact-induced loss of primordial noble gases from experimentally shocked Allende meteorite (abstract). 22nd NIPR Symposium on Antarctic Meteorites. pp. 135–136.

Ott U., Mack R., and Chang S. 1981. Noble-gas-rich separates from the Allende meteorite. *Geochimica et Cosmochimica Acta* 45: 1751–1788.

Ozima M. and Podosek F. A. 2002. *Noble gas geochemistry*, 2nd ed. Cambridge: Cambridge University Press. 286 p.

Pepin R.O., Becker R. H., and Rider P. E. 1995. Xenon and krypton isotopes in extraterrestrial regolith soils and in the solar wind. *Geochimica et Cosmochimica Acta* 59:4997–5022.

Russell S. S., Zipfel J., Folco L., Jones R., Grady M. M., McCoy T., and Grossman J. N. 2003. The Meteoritical Bulletin, No. 87. *Meteoritics & Planetary Science* 38:A209.

Scherer P. and Schultz L. 2000. Noble gas record, collisional history, and pairing of CV, CO, CK, and other carbonaceous chondrites. *Meteoritics & Planetary Science* 35:145–153.

Schultz L., Funk H., Nyquist L., and Signer P. 1971. Helium, neon and argon in separated phases of iron meteorites. *Geochimica et Cosmochimica Acta* 35:77–88.

Scherstén A., Elliott T., Hawesworth C. , Russell S., and Masarik J. 2006. Hf-W evidence for rapid differentiation of iron meteorite parent bodies. *Earth and Planetary Science Letters* 241: 530–542.

Scott E. R. D. and Wasson J. T. 1975. Classification and properties of iron meteorites. *Reviews of Geophysics and Space Physics* 13: 527–546.

Srinivasan B., Lewis R. S., and Anders E. 1975. Origin of noble gases in Allende, I. Host phases of fission xenon and other gases. *Meteoritics* 10:491–492.

Ulff-Møller F. 1998. Solubility of chromium and oxygen in metallic liquids and the co-crystallization of chromite and metal in iron meteorite parent bodies (abstract #1969). 29th Lunar and Planetary Science Conference. CD-ROM.

Voshage H. 1984. Investigations on cosmic-ray-produced nuclides in iron meteorites, 6. The Signer-Nier model and the history of the cosmic radiation. *Earth and Planetary Science Letters* 71:181–194.

Voshage H. and Feldmann H. 1979. Investigations on cosmic-ray-produced nuclides in iron meteorites, 3. Exposure ages, meteoroid sizes and sample depths determined by mass spectrometric analyses of potassium and rare gases. *Earth and Planetary Science Letters* 45:293–308.

Wada N. and Matsuda J. 1998. A noble gas study of cubic diamonds from Zaire: Constraints on their mantle source. *Geochimica et Cosmochimica Acta* 62:2335–2345.

Wieler R., Anders E., Baur H., Lewis R. S., and Signer P. 1992. Characterisation of Q-gases and other noble gas components in the Murchison meteorite. *Geochimica et Cosmochimica Acta* 56: 2907–2921.